Mazurek-Budzynska, M.; Behl, M.; Razzaq, M.Y.; Noechel, U.; Rokicki, G.; Lendlein, A.:
Hydrolytic stability of aliphatic poly(carbonate-urea-urethane)s: Influence of hydrocarbon chain length in soft segment.
In: Polymer Degradation and Stability. Vol. 161 (2019) 283 - 297.
First published online by Elsevier: 28.01.2019

https://dx.doi.org/10.1016/j.polymdegradstab.2019.01.032

Hydrolytic stability of aliphatic poly(carbonate-urea-urethane)s: Influence of hydrocarbon chain length in soft segment

Magdalena Mazurek-Budzyńska[1,2,*], Marc Behl[1,3], Muhammad Y. Razzaq[1], Ulrich Nöchel[1], Gabriel Rokicki[2], Andreas Lendlein[1,3]

[1] *Institute of Biomaterial Science, Helmholtz-Zentrum Geesthacht, Kantstr. 55, 14513 Teltow, Germany*

[2] *Department of Chemistry, Warsaw University of Technology, Noakowskiego 3, 00-664 Warsaw, Poland*

[3] *Institute of Chemistry, University of Potsdam, Karl-Liebknecht-Str. 24-25, 14476 Potsdam, Germany*

** Corresponding author: magdalena.mazurek-budzynska@hzg.de*

Abstract

Poly(carbonate-urethane)s (PCUs) exhibit improved resistance to hydrolytic degradation and in *vivo stress* cracking compared to poly(ester-urethane)s and their degradation leads to lower inflammation of the surrounding tissues. Therefore, PCUs are promising implant materials and are considered for devices such as artificial heart or spine implants. In this work, the hydrolytic stability of different poly(carbonate-urethane–urea)s (PCUUs) was studied under variation of the length of hydrocarbon chain (6, 9, 10 and 12 methylene units) between the carbonate linkages in the precursors. PCUUs were synthesized from isophorone diisocyanate and oligo(alkylene carbonate) diols using the moisture-cure method. The changes of sample weight, thermal and mechanical properties, morphology, as well as the degradation products after immersion in a buffer solution (PBS, pH = 7.4) for up to 10 weeks at 37 °C were monitored and analyzed. In addition, mechanical properties after 20 weeks (in PBS, 37 °C)

were investigated. The gel content was determined based on swelling experiments in chloroform.

Based on the DSC analysis, slight increases of melting transitions of PCUUs were observed, which were attributed to structure reorganization related to annealing at 37 °C rather than to the degradation of the PCUU. Tensile strength after 20 weeks of all investigated samples remained in the range of 29 to 39 MPa, whereas the elongation at break ε_m decreased only slightly and remained in the range between 670 and 800%. Based on the characterization of degradation products after up to 10 weeks of immersion it was assessed that oligomers are mainly consisting of hard segments containing urea linkages, which could be assigned to hindered-urea dissociation mechanism. The investigations confirmed good resistance of PCUUs to hydrolysis. Only minor changes in the crystallinity, as well as thermal and mechanical properties were observed and depended on hydrocarbon chain length in soft segment of PCUUs.

Keywords: Poly(carbonate-urea-urethane)s, hydrolytic stability, degradation

1. Introduction

Poly(carbonate-urethane)s (PCUs) synthesized from oligocarbonate diols as soft segment precursors represent a very fast developing group of materials used in medical applications such as meniscus or spine implants, artificial heart, or pacemaker lead insulation [1-3]. According to *in vitro* and early *in vivo* studies, PCUs exhibit improved resistance to hydrolytic degradation and stress cracking (*in vivo*) when compared to medical grade poly(ester-urethane)s [4-7]. It is known already since the 1970's that the hydrolytic degradation of PCUs proceeds without catalytic effect of acidic degradation products, therefore, a local decrease of

pH and resultant inflammation of the surrounding tissues are much lower than in case of poly(ester-urethane)s [8].

PCUs were initially prepared from aromatic diisocyanates such as toluene diisocyanate (TDI) and 4,4'-methylene diphenyl diisocyanate (MDI) [9-12]. However, the aliphatic PCUs exhibited higher stability to oxygen when compared to aromatic-based PCUs, and the aliphatic degradation products were less toxic than those resulting from aromatic diisocyanates [9, 13]. Therefore, due to the potential usage in coatings and biomedical applications, PCUs obtained from the aliphatic [1, 14-18] and cycloaliphatic [2, 18] diisocyanates gained attention of scientists and the industry. Furthermore, PCUs based on cycloaliphatic diisocyanates were very resistant to hydrolysis due to the high stiffness of the aliphatic rings among the hard segments, which hindered the access of water molecules into the polymer chains [9, 19, 20]. In addition, it was found that the degree of hydrogen bonding among the carbonate and urethane linkages is a significant factor, which contributes to the hydrolytic stability of PCUs [20, 21]. Furthermore, *in vitro* studies have shown that vascular grafts made of this poly(carbonate-urea-urethane) are mechanically stable in terms of exposure to static hydrolytic, oxidative, peroxidative and alfa-2-macroglobulin degradation [22].

It has been reported that the length of hydrocarbon chain, as well as odd/even CH_2 units content, strongly influences the morphology of poly(carbonate-urea-urethane)s (PCUUs) (e.g. crosslinking density, degree of crystallinity). Therefore, we hypothesized that the concentration of carbonate units within the soft segments will have significant influence on hydrolytic stability of the investigated materials. In previous studies, differences between hydrolytic stability of PCUUs based on oligocarbonate diols containing up to 6 methylene units between the carbonate linkages have been investigated, showing significant influence of concentration of polar carbonate groups in the polymer structure [2]. However, data describing hydrolytic stability of PCUUs based on oligocarbonate diols containing longer hydrocarbon chains were

not reported so far. Therefore, the aim of this study was to investigate the hydrolytic stability of aliphatic PCUUs prepared from oligocarbonate diols (OCD) containing longer hydrocarbon chains (6, 9, 10, and 12 methylene units).

PCUUs were synthesized by using the moisture-cure method, utilizing cycloaliphatic isophorone diisocyanate. The changes of the sample weight, gel content, thermal and mechanical properties, as well as morphology of the samples after immersion in a buffer solution (PBS, pH = 7.4) up to 20 weeks at 37 °C were monitored and the degradation products were analyzed. Crystallinity of samples was investigated by means of differential scanning calorimetry (DSC) and small angle X-ray scattering (SAXS), whereas mechanical properties were monitored by dynamic mechanical thermal analysis (DMTA) and tensile testing. Furthermore, infrared spectroscopy (FTIR) and magnetic resonance spectroscopy (NMR) were used to control the potential changes of chemical structure of the investigated samples. In addition, degradation products (if any) were investigated by means of FTIR, gel permeation chromatography (GPC), and NMR analyses.

2. Experimental

2.1. Materials

Phosphate Buffered Saline (PBS, pH= 7.4) (Gibco, USA), Chloroform (purity ≥ 99.9%), *d*-Chloroform ($CDCl_3$) (purity ≥ 99%) (Roth, Germany), 1,10-decanediol (purity 98%), dimethyl carbonate (DMC) (purity 99%), 1,12-dodecanediol (purity ≥ 98.0%), isophorone diisocyanate (IPDI) (purity 98%), 1,6-hexanediol (purity 98%), 1,9-nonanediol (purity 98%), titanium(IV) butoxide (purity ≥ 97%) (Sigma-Aldrich, Poznan, Poland) were used as received.

2.2. Synthesis of poly(carbonate-urea-urethane) networks

PCUUs were synthesized using the moisture-cure method from isophorone diisocyanate and oligo(alkylene carbonate) diols as precursors [23]. In the first step diisocyanate telechelics were obtained by reacting various oligo(alkylene carbonate) diols (average M_n = 3000 ± 500

g·mol^{-1}) with an excess of isophorone diisocyanate (IPDI). Subsequently, the curing mixture was poured into glass mold and cured in a climate chamber (Binder GmbH, Tuttlingen, Germany) under controlled conditions of humidity and temperature.

PCUUs were named **PCUU-X**, where **X** is 6, 9, 10, or 12 representing the number of methylene groups between carbonate groups within the oligo(alkylene carbonate) diol (soft segment of PCUU). PCUUs immersed in PBS buffer were named **PCUU-X-PBS_Y**, where **Y** represents time, for which the sample was immersed in buffer (in weeks). Reference samples were named **PCUU-X_Y**.

2.3. Characterization techniques

^{1}H NMR and ^{13}C NMR spectra were acquired on a DRX 500 Avance spectrometer (Bruker, Rheinstetten, Germany) at 298 K using tetramethylsilane as an internal reference and $CDCl_3$ as a solvent, and were analyzed with MestReNovav.6.2.0-7238 (Mestrelab Research S.L, Santiago, Spain) software. The error of the method was estimated based on the error of the integral peak area (around 5%).

Multidetector GPC measurements were performed at a solvent flow rate of 1 mL·min^{-1} at 35 °C using chloroform as an eluent and 0.2 wt% toluene as internal standard. The system was equipped with a precolumn, two 300 mm x 8.0 mm linear M columns (Polymer Standards Service GmbH (PSS), Mainz, Germany), an isocratic pump 2080, an automatic injector AS 2050 (both Jasco, Tokyo, Japan), a refractive index detector (Shodex RI-101, Munich, Germany), and a differential viscometer/light scattering dual detector T60A (Viscotek Corporation, Houston, USA). The SEC software WINGPC 6.2 (PSS) was used to determine the molecular weight distributions by universal calibration with polystyrene standards (PSS). The error of the measurement method was estimated as 10% based on measurements of PS standards.

FTIR spectra of non-soluble samples were recorded at room temperature on a Nicolet FTIR-6700 (Thermo Scientific, Karlsruhe, Germany) with SensIR Diamant H-ATR (Resultec, Illerkirchberg, Germany), using a spectral width ranging from 600 to 4000 cm^{-1}, 4 cm^{-1} resolution, 50 scans. Soluble samples of degradation products as well as extracted fractions of PCUUs were measured in the transmission mode, in which solutions in chloroform were placed on KBr-pallets.

Dynamic mechanical thermal analyses (DMTA) at varied temperatures were conducted with a Gabo (Ahlden, Germany) Eplexor 25 N. All experiments were performed in temperature sweep mode with a constant heating rate of 3 $K \cdot min^{-1}$ and an oscillation frequency of 1 Hz. Samples were investigated in a temperature interval from -100 to 200 °C.

DSC experiments were conducted on a Netzsch DSC 204 Phoenix (Selb, Germany). All experiments were performed with a constant heating and cooling rate of 10 $K \cdot min^{-1}$ and with a waiting period of 2 min at the maximum and minimum temperature. Samples were investigated in the temperature range from -100 to 150 °C, at first heated from 0 to 150 °C, then cooled to -100 °C and again heated to 150 °C. Both melting temperature and glass transition temperature were determined based on the heating curves, whereas the crystallization temperature was determined based on the cooling curve.

Small-angle X-ray scattering (SAXS) was performed on a Bruker (Karlsruhe, Germany) Nanostar diffractometer, operating 40 kV and 35 mA on a copper anode. Point focused X-rays were monochromated and parallelized by Montel-optics and collimated by a 750/400/1000 µm 3-pinhole combination, thus a 400 µm beam having a wavelength of 0.15418 nm (CuKα) was obtained. The sample to detector distance was 1070 mm calibrated with a silver behenate standard. A Vantec-2000 detector (Bruker, Karlsruhe, Germany) (2048 x 2048 pixel, 68 µm pixel size) was employed to record scattered intensities, the primary beam was stopped (6 mm lead beam-stop) close before the detector. The primary and secondary beam paths as well as

the sample chamber were operated under vacuum (~10^{-3} mbar). Samples were placed into a small powder-sample holder (0.2 mm thickness) and exposed 1 h to obtain a two dimensional scattering pattern, which was corrected for spatial distortion and background subtracted (weighted with sample transmission). Isotropic scattering patterns were integrated (azimuthal average over 360°) by 5-point binning with a 0.001° (2θ) step size from 2θ = 0.1° to 3.2° leading into one-dimensional scattering curves of scattered intensity *vs*. scattering angle (*I vs*. 2θ). Anisotropic scattering patterns were integrated over a 10° wide azimuthal range along the axis of symmetry (fiber axis, s_3). The scattering angle was converted into scattering vector **s**, being $|\mathbf{s}| = s = (2/\lambda)\sin\theta$ and a Kratky-plot (Lorenz correction Is^2 *vs*. *s*) was utilized to extract the long period *L* from the position of the peak maxima as $L = s^{-1}$.

Tensile tests were conducted with standard samples (ISO 527-2/1BB) cut from films on a tensile tester Z75 (Zwick, Ulm, Germany) equipped with thermo-chamber (Zwick, Ulm, Germany), temperature controller Eurotherm control 2408 (Eurotherm Regler, Limburg, Germany), and load cells suitable to determine maximum forces of 200 N (Zwick, Ulm, Germany). The strain rate in uniaxial tensile test was 20 mm·min^{-1}.

The gel fraction content (G_F) and the mass equilibrium degrees of swelling (Q_m) were determined by swelling the films in 200-fold excess (related to the sample weight) of chloroform for 72 hours at room temperature and subsequent drying. Endpoints of swelling and drying were reached when constant weights were obtained. The G_F values were calculated as the ratio of the weights of the non-swollen (m_d) and the extracted (m_{ex}) sample according to equation 1 [24]. Furthermore, swollen samples were removed and the solutions containing the soluble fractions were analyzed by means of GPC, ^{1}H and ^{13}C NMR, and FTIR.

$$G_F = \frac{m_{ex}}{m_d} \qquad (1)$$

The mass equilibrium degrees of swelling (Q_m) were estimated by comparing weights of the non-swollen samples (m_d) and in the swollen state (m_{sw}) according to equation (2) [25].

$$Q_m = \frac{m_{sw} - m_0}{m_d} \qquad (2)$$

2.4. Hydrolytic stability measurements

Standard samples (according to standard ISO 527-2/1BB) were cut from films and dried at 25 °C under vacuum for 24 h. Then they were weighted (m_0), placed in plastic vials with 2 cm^3 of buffer and stored in an oven at 37 °C for a predefined period. Afterwards samples were washed with distilled water (3 times within 24h) and weighted (m_s) to calculate the water uptake (eq. (3)) and then dried under vacuum at 30 °C until the weight was constant (m_d). The weight loss was calculated according to equation (4). For each type of the polymer, six samples were used and the average values of water uptake and weight loss with standard deviations were calculated (eq. 5).

$$water\ uptake\ (\%) = \frac{m_s - m_0}{m_0} x\ 100 \qquad (3)$$

$$weight\ loss\ (\%) = \frac{m_0 - m_d}{m_0} x100 \qquad (4)$$

In addition, three samples of each type were used as reference specimen. They were stored in the same conditions of temperature and pressure but without addition of PBS buffer (Figure 1).

To investigate degradation products of PCUUs, solutions of PBS buffer, in which samples were immersed, were analyzed for a content of organic compounds. After removal of the sample, solution was freeze-dried for 48 h, and the residue dissolved in chloroform. After filtration of the solution, FTIR, GPC, and ^{1}H NMR analyses were performed.

If not mentioned otherwise, the errors of the measurements were calculated based on the average value of results of three to six samples of each composition. The standard deviations (σ) were calculated based on equation (5), where x is an average value of all results and n is number of samples.

$$\sigma = \sqrt{\frac{\Sigma(x-\overline{x})^2}{n}} \qquad (5)$$

Schematic presentation of performed experiments is shown in the Figure 1.

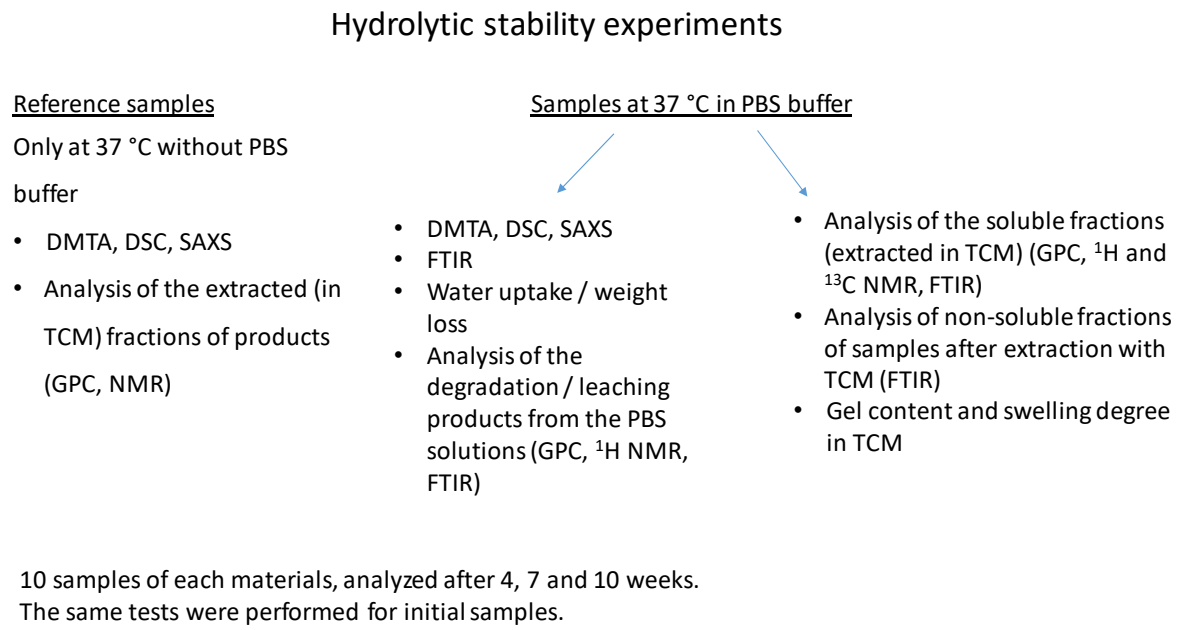

Figure 1. Schematic presentation for performed experiments of hydrolytic stability of PCUUs.

3. Results and Discussion

In the presented study, the hydrolytic degradation of various PCUUs based on aliphatic oligo(alkylene carbonate) diols of different length of hydrocarbon chain were investigated (Scheme 1). The changes of the investigated PCUU properties such as sample weight (water uptake and weight loss), the morphology, gel content, as well as the thermal properties after immersion in a buffer solution (PBS, pH = 7.4) for up to 10 weeks at 37 °C were monitored and analyzed. In addition, mechanical tests of samples after 4 and 20 weeks in PBS buffer at 37 °C were performed. For better understanding of the composition differences in oligocarbonate diols as well as in PCUUs, detailed compositions are presented in Table 1.

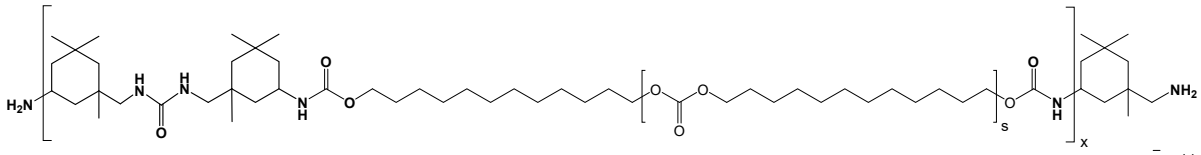

PCUU-12, based on oligo(dodecamethylene carbonate) diol

$\bar{s} = 11$

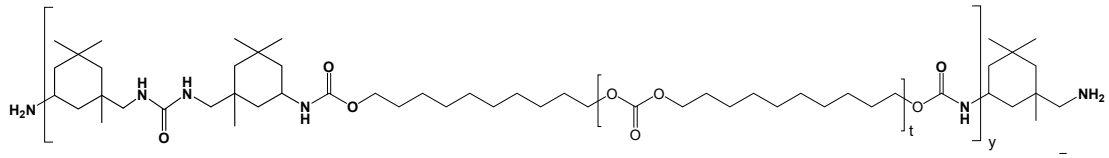

PCUU-10, based on oligo(decamethylene carbonate) diol

$\bar{t} = 16$

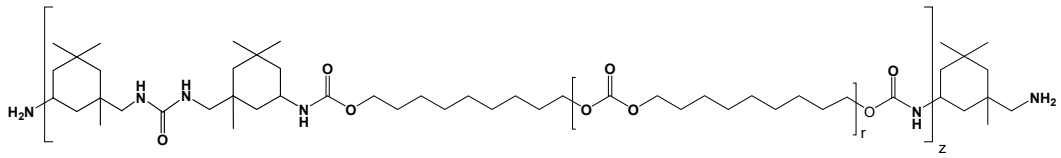

PCUU-9, based on oligo(nonamethylene carbonate) diol

$\bar{r} = 14$

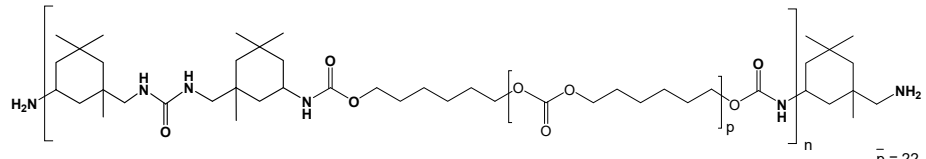

PCUU-6, based on oligo(hexamethylene carbonate) diol

$\bar{p} = 22$

Scheme 1. Simplified structures of PCUUs based on various oligo(alkylene carbonate) diols.

Longer blocks of hard segments are also possible to be formed during the synthesis (Scheme 2). Average numbers of repeating units in oligo(alkylene carbonate)s were marked as $\bar{s}$, $\bar{t}$, $\bar{r}$, and $\bar{p}$ in case of PCUU-12, PCUU-10, PCUU-9, and PCUU-6, respectively.

Table 1. The composition of investigated PCUUs.

Sample	M_n of oligo(alkylene carbonate) diol [a]	Content of hard segments in PCUUs [b]		Molar ratio of carbonate / urethane / urea groups in PCUUs [b]
	(g·mol^{-1})	(mol.%)	(wt.%)	
PCUU-6	3300 ± 300	75 ± 1	17 ± 1	22 / 2 / 2
PCUU-9	2800 ± 300	75 ± 1	19 ± 1	14 / 2 / 2
PCUU-10	3400 ± 300	75 ± 1	17 ± 1	16 / 2 / 2
PCUU-12	2800 ± 300	75 ± 1	19 ± 1	11 / 2 / 2

[a] Determined by means of ^{1}H NMR spectroscopy using $CDCl_3$ as a solvent.

[b] Calculated based on the amount of oligo(alkylene carbonate) diols and IPDI used for the synthesis of PCUUs.

3.1. Weight changes

The uptake of water occurs firstly when exposing the polymers to aqueous media and mostly depends on the hydrophilicity of the material. The weight of the samples did not change significantly within the investigated period and the weight gain was below 1 wt% for all investigated samples (Figure 1, Table S1). The highest water uptake (up to 0.9 ± 0.5%) was observed for PCUU-6, which was the most hydrophilic PCUU among the investigated materials (the shortest hydrocarbon chain in the soft segment) (Figure 2). In case of PCUU-9, PCUU-10, and PCUU-12 the average water uptake decreased with the time of immersion in PBS solution (for example in case of PCUU-10 it dropped from 0.7 ± 0.5% to 0.2 ± 0.5%). Average weight loss was around 0.2-0.3 ± 0.5% in case of all investigated samples after 10 weeks of immersion in PBS solution (Figure S2, Table S1). However, it has to be underlined that these results (weight change in the range of 0.0-0.2 mg) are in range of measurement error.

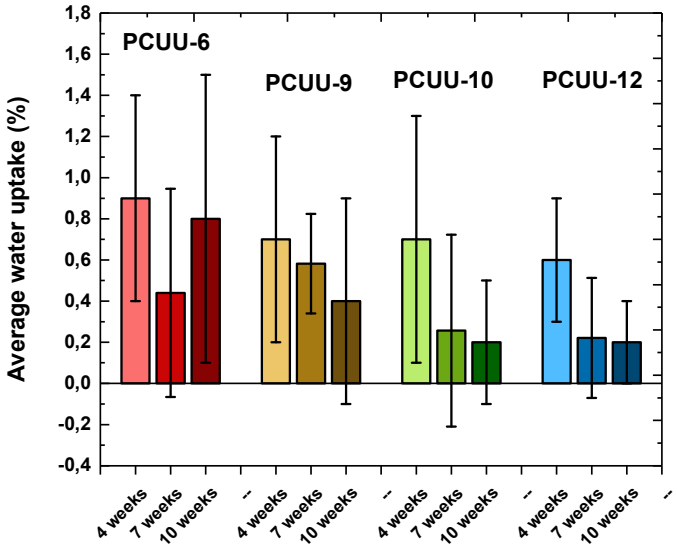

Figure 2. Average water uptake of investigated PCUUs after immersion in PBS solution at 37 °C after 4, 7, and 10 weeks.

3.2. FTIR analysis

The FTIR spectra of obtained PCUUs are shown in Figure 3. In the spectra of initial sample no absorption bands characteristic for NCO groups (2260 cm^{-1}) were observed, indicating complete conversion of the NCO group. The region between 3200 and 3500 cm^{-1} is assigned to N-H stretching bands. The broad absorption bands 2800–3000 cm^{-1} correspond to the stretching vibration of CH_2 groups. The wave numbers of asymmetric and symmetric stretching bands for PCUU based on 1,12-dodecanediol (PCUU-12), 1,10-decanediol (PCUU-10), and 1,9-nonanediol (PCUU-9) were 2922 and 2852 cm^{-1}, respectively. In case of PCUU-6 asymmetric and symmetric stretching bands were shifted to 2939 cm^{-1}, which can be attributed to conformational ordering during crystallization of the soft segments caused by the decrease of methylene groups number in the soft segment phase [23]. In the range of 1620–1780 cm^{-1} the bands of carbonyl groups were observed as follows: amide I (non-hydrogen bonded urethane around 1700 cm^{-1} and hydrogen-bonded urethane around 1690 cm^{-1}), carbonate (hydrogen-bonded around 1720 cm^{-1} and non-hydrogen bonded around 1740 cm^{-1}), and hydrogen-bonded urea carbonyl band at nearly 1630 cm^{-1} [26]. Amide II bands from urethane and urea could also be identified in the spectra and located around 1520-1565 cm^{-1}.

In case of PCUU-6 and PCUU-9, no changes in the FTIR spectra were found after immersion in PBS buffer, independently from the time of immersion (Figure 3a and b). In case of PCUU-10 and PCUU-12, significant intensity increase of characteristic bands of the amide groups from urethane and urea ones (at 1560 and 1636 cm^{-1}) were observed (Figure 3c and d). This could suggest that within the time when the samples were immersed in PBS solutions reaction of chain extension with water continued, resulting in the formation of new urea groups. Most probably, reaction with water of less hydrophilic, containing more crystalline phase PCUU-10 and PCUU-12 ($\Delta H_m = 30 \pm 1$ $J \cdot g^{-1}$) proceeds slower than in case of more hydrophilic PCUU-6, or less crystalline PCUU-9 ($\Delta H_m = 18 \pm 1$ $J \cdot g^{-1}$). Therefore, initial materials after equal time of reaction with water were not cured to the same extent [2].

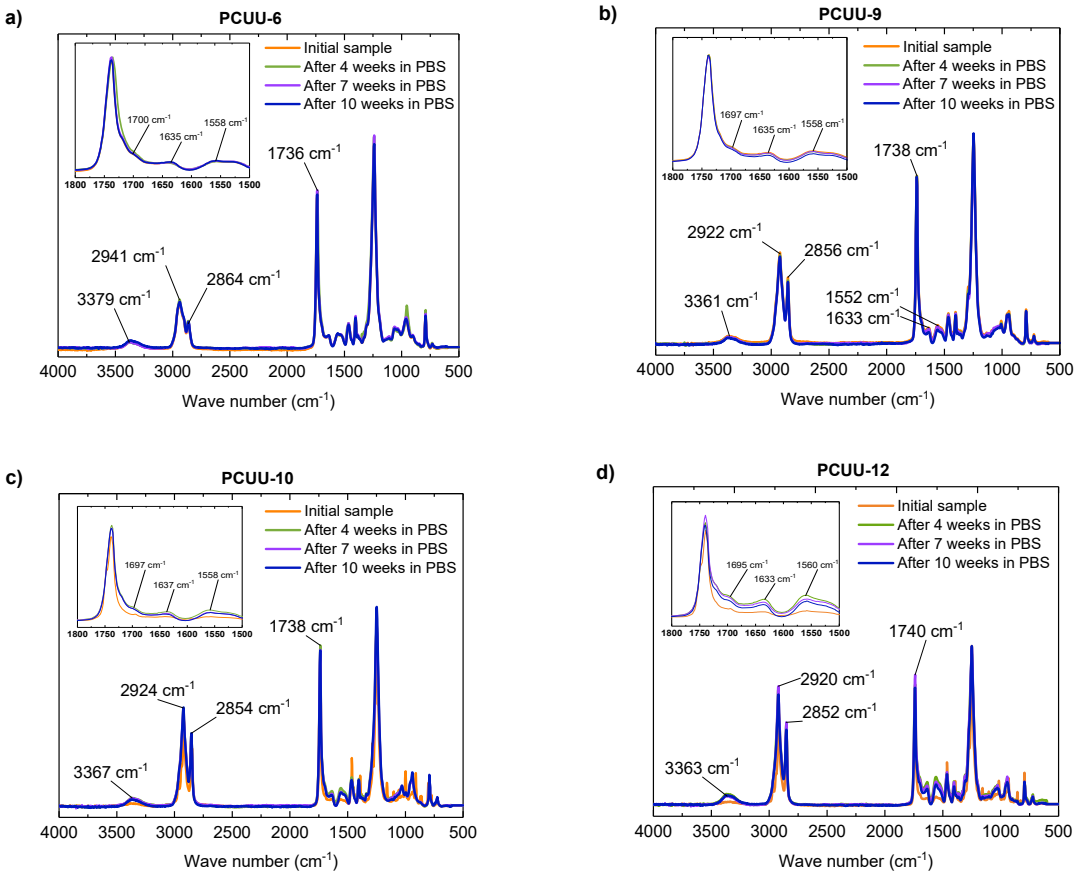

Figure 3. FTIR spectra of PCUUs before and after immersion in PBS solution for 4, 7, and 10 weeks. PCUU-6 (a), PCUU-9 (b), PCUU-10 (c), PCUU-12 (d).

3.3. Gel content and degree of swelling in chloroform

Crosslinking densities were measured after each period of immersion in PBS solutions as well as for the initial materials (Figure 4, Table S1) by determining the gel content and swelling ratios in chloroform (TCM). The highest swelling ratios in TCM (around 4000%) and simultaneously the lowest gel contents (around 65-70%) were observed in case of PCUU-6. In case of PCUU-10 and PCUU-12 the gel content and swelling ratios were almost the same - around 97% and around 1500%, respectively). The lowest swelling ratio (around 1200%) was observed in case of PCUU-9 and slightly decreased within the time of immersion in PBS solution. This could be the result of the odd number of methylene groups in the oligocarbonate

chains, which leads to a different spatial arrangement of the polymer chains. It was previously reported that in case of PCUUs the degree of phase separation is higher in case of samples based on oligocarbonate diols containing odd number of methylene groups [23]. This can result in a higher content of hydrogen bonds and decrease the degree of swelling. The gel content of PCUU-9 was the same as in case of PCUU-10 and PCUU-12, and slightly increased with the increase of the time of immersion in PBS solution.

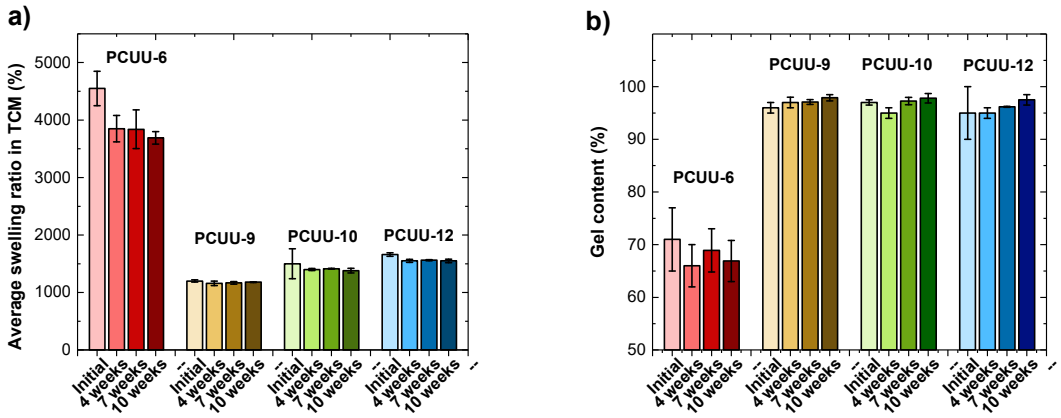

Figure 4. Average swelling ratio in chloroform (TCM) (a) and gel content (b) of investigated poly(carbonate-urea-urethane)s before and after immersion in PBS buffer for 4, 7, and 10 weeks.

Due to high differences between gel content of PCUU-6 and the other samples, extracted fractions of samples were analyzed also by means of NMR spectroscopy (Figures 5-6). The crucial point was to see whether there is any difference in the chemical structure of PCUU-6 in comparison to other investigated PCUUs, which could affect solubility of PCUU-6 (for example content of covalent crosslinks based on allophanate/biuret groups).

Signals characteristic for allophanate formations, typically located in ^{1}H NMR spectra at around 11-12 ppm, were not observed in the spectra of extracts of all of the investigated samples (Figure 5-6). However, it might be related to a very low concentration of the crosslinks within the polymer structure (extracted fraction), for which the sensitivity of NMR

spectroscopy is not sufficient. Signals of NH protons in urethane and urea groups at 7.0-8.0 pm (signals 'a', Figure 5a) and at 5.5-6.5 ppm (signals 'b', Figure 5b), were observed. In addition, the following signals were detected: at 4.0 ppm (signals 'c') assigned to characteristic signals for CH_2- in the direct connection with carbonate group, at 3.9 ppm (signals 'd') C**H$_2$**-O(O)C-NH- connected with urethane group, at 3.7-3.5 ppm (signals 'e') CH_2- in the direct connection with -NH- of urethane group, and at around 3.16 ppm (signals 'f') CH_2- in the direct connection with -NH- in the urea group (Figure 5) [27-31]. However, based on ^{1}H NMR spectra, the differences, which could explain the different behavior of PCUU-6 in comparison to other PCUUs could not be distinguished (Figure 6). Due to the lower sensitivity of ^{13}C NMR, measurement was only possible in case of PCUU-6, which was soluble in higher extend, however signals related to urea and urethane protons are too small for complex interpretation [32-36] (Figure 7).

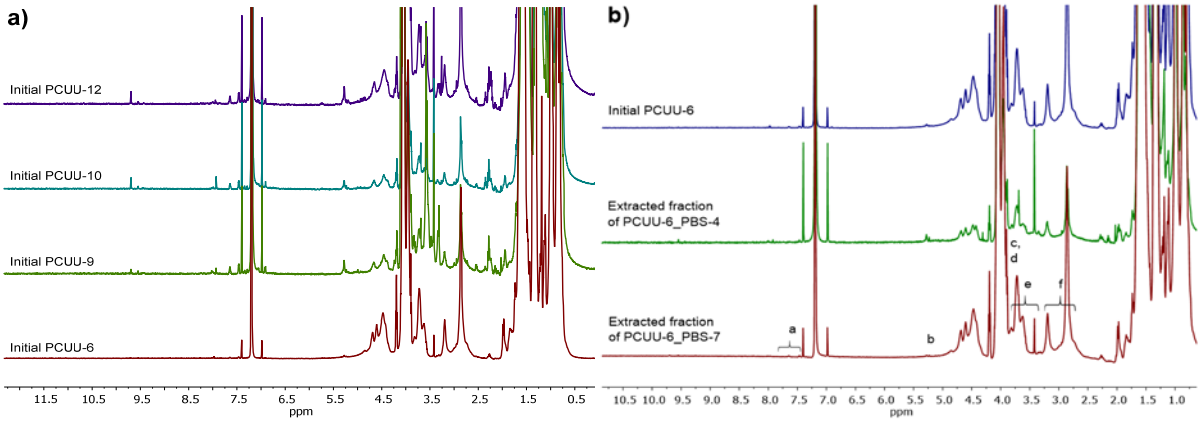

Figure 5. ^{1}H NMR spectra (500 Hz, $CDCl_3$) of soluble fractions of all initial PCUUs (a) and of PCUU-6, PCUU-6_PBS-4 and PCUU-6_PBS-7 (b).

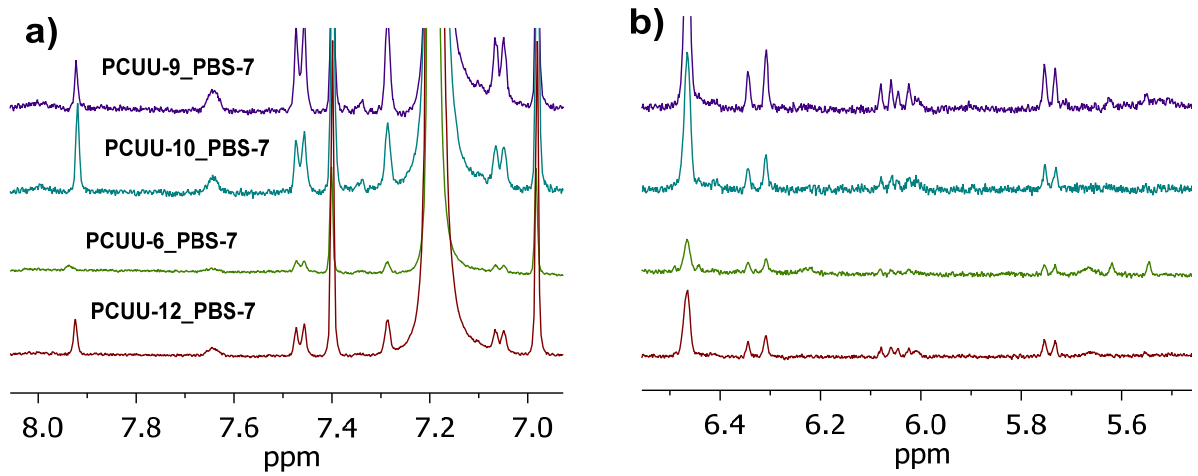

Figure 6. ^{1}H NMR spectra (500 Hz, $CDCl_3$) of soluble fractions of PCUU-9_PBS-7, PCUU-10_PBS-7, PCUU-6_PBS-7, and PCUU-12_PBS-7 ranging from 7 to 8 ppm (a) and from 5.5 to 6.5 ppm (b).

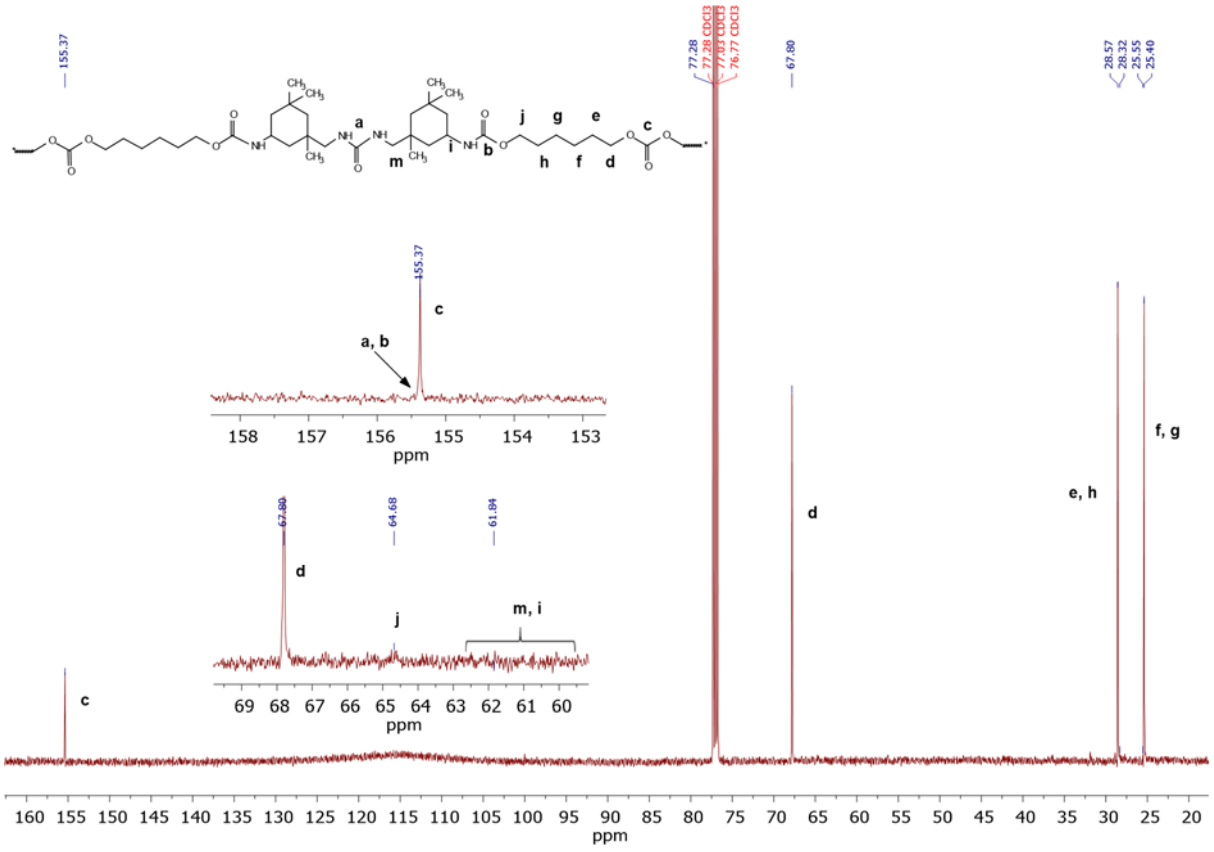

Figure 7. ^{13}C NMR spectrum (500 Hz, $CDCl_3$) of soluble fraction of PCUU-6.

FTIR analysis did not show any differences in the structure of soluble fraction of polymers before and after immersion, as well as within various time of immersion in PBS solution (Figure 8a, exemplarily for PCUU-6). Slightly higher signals of amide II bands were observed in FTIR spectra in case of non-soluble fractions of samples when compared to soluble ones (Figure 8b, exemplarily for PCUU-10). Also the maximum of the peak related to carbonyl band was shifted from 1738 to 1745 cm^{-1}, which suggests a lower content of hydrogen bonds in the soluble fraction of the polymer.

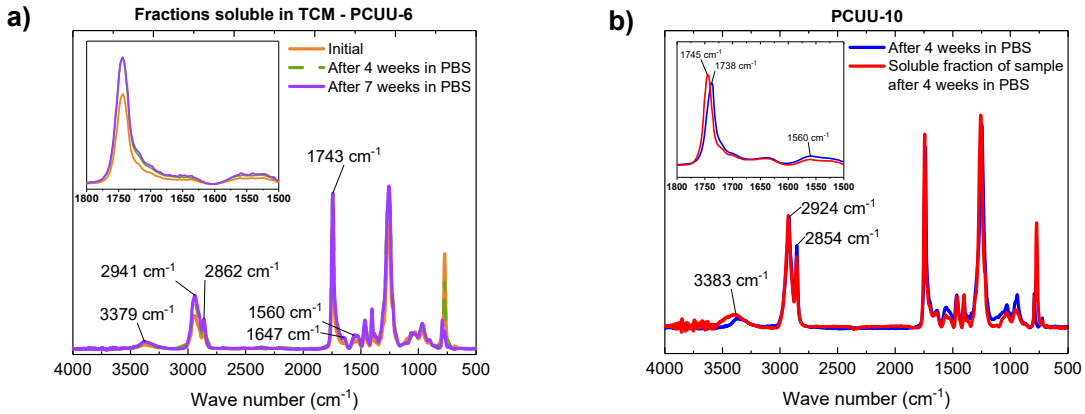

Figure 8. FTIR spectra of soluble fractions of PCUU-6 before and after immersion in PBS buffer for 4 and 7 weeks (a). FTIR spectra of soluble and non-soluble fractions of samples PCUU-10_PBS-4 (b).

3.4. Changes of the thermal properties and microstructure

To see whether immersion in PBS buffer can influence the microstructure of the investigated materials, thermal properties by means of DSC and DMTA, as well as the change of the long period by means of SAXS were assessed. An increase of the melting point of PCUUs was observed in the first heating curve (Figure 9). In case of PCUU-6, PCUU-9, and PCUU-10 the splitting of the original peaks were observed when new endothermal peaks formed around 40 °C. Most probably, this behavior can be explained by temperature-induced phase segregation of the domains provided by soft segments of polycarbonate sequences into

more organized and stable crystalline forms in addition to the amorphous domains [1]. The most pronounced peak was observed in case of PCUU-9 (ΔH_m= 3-7 J·g^{-1}) (Figure 9b), which could be related to the different spatial arrangements of the polymer chains due to the odd number of methylene groups in the soft segment. To distinguish whether the observed changes are related only to reorganization of soft segment domains and are not caused by PBS solution, the reference samples, which were stored at 37 °C without PBS solutions were analyzed. Thermal properties of samples stored at 37 °C and the one stored at 37 °C in PBS solutions almost did not show differences in the first heating scans (Figure 10, exemplarily for samples after 4 weeks in PBS solutions), which indicates that co-crystallization of the amorphous part of oligocarbonate segment occurred due to annealing at 37 °C. These results are in agreement with previously published results of hydrolytic degradation (37 °C, PBS) of poly(carbonate-urethane)s made from diisocyanate-1,6-hexane and butane-1,4-diol. Changes of the melting enthalpies did not change significantly (increase of 6-9%) in case of all investigated samples (Figure 9, Table S1), which means that the content of crystalline phase did not increase during immersion in PBS buffer. The long period measured by SAXS increased slightly with the time of immersion, most pronounced in case of PCUU-9 (Figure 11, Table S3), which confirms reorganization of the crystalline and amorphous phases attributed to the soft segment.

Furthermore, second heating scans in DSC diagrams did not show additional crystalline phase, which confirms that changes in the thermal transitions were caused by an annealing process rather than hydrolytic degradation in the presence of PBS solution. Detailed values of all thermal transitions and enthalpies are listed in Table S2.

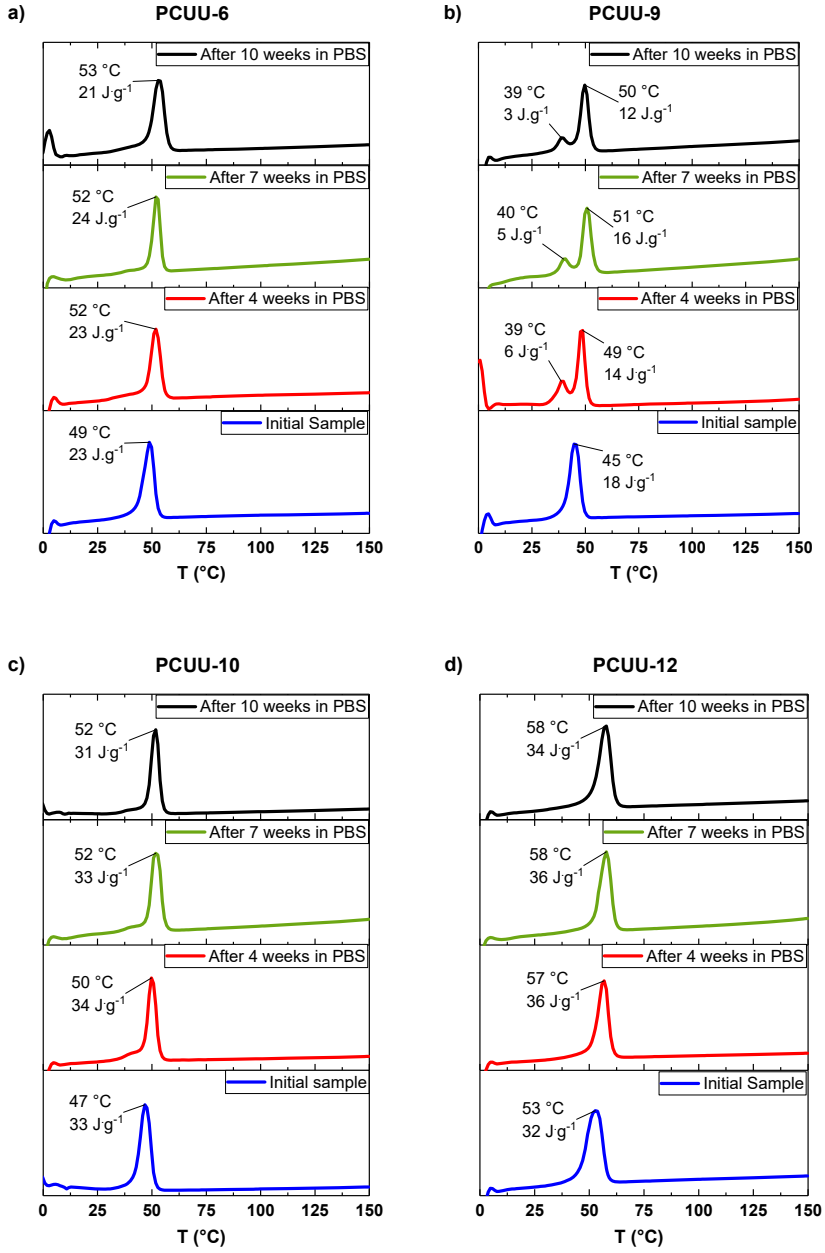

Figure 9. DSC thermograms of PCUUs before and after immersion in PBS buffer for 4, 7, and 10 weeks – first heating curves.

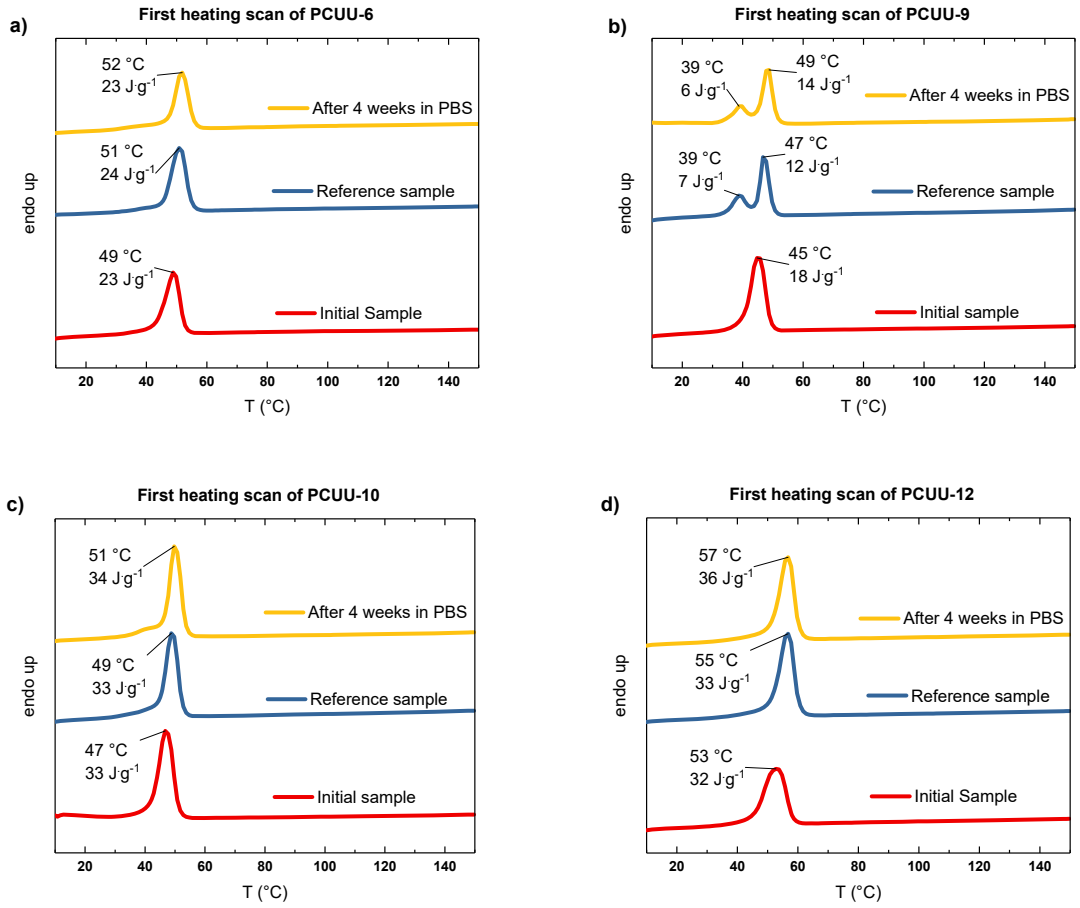

Figure 10. DSC first heating curves of PCUUs before and after immersion in PBS buffer for 4 weeks and the reference samples, which were not stored at PBS solutions (only at 37 °C).

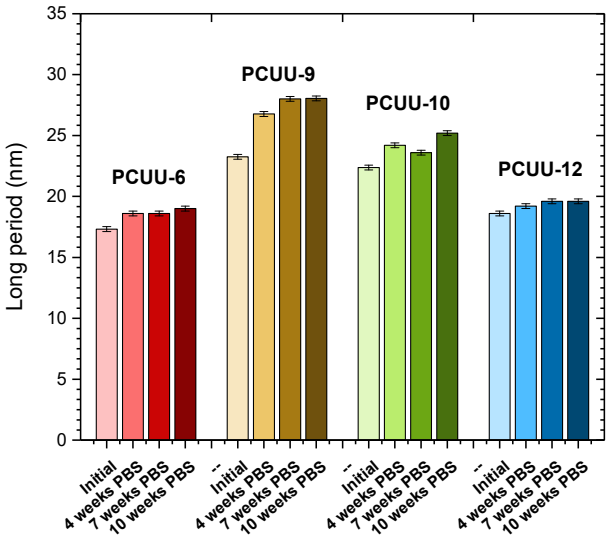

Figure 11. Long period of PCUUs before after immersion in PBS buffer measured by SAXS.

Results of dynamic mechanical thermal analysis, in agreement with DSC result, showed a slight increase of T_m. In case of sample PCUU-10 curves of initial, reference, and immersed in PBS solution samples were almost completely overlapping (Figure 12c, Figure S4). Minor changes of the T_g, visible also in DSC curves (Table S2), could be related to the small remaining traces of water remained in the samples. In case of PCUU-9 the storage modulus (E') increased in the range of T < T_m from 940 to 1500 MPa at -100 °C and at 20 °C from 50 MPa to 77 MPa (Figure 12b) after 10 weeks in PBS solution at 37 °C. In contrast, in case of PCUU-6 at -100°C the E' decreased from 2500 MPa to 1900 MPa, and at 20 °C from 190 MPa to 130 MPa (Figure 12a). Elastic plateau regions of all investigated samples remained unchanged, which also proves that changes of the properties of the material are related to reorganization of the crystalline phase contributed by the soft segments, and that above T_m the thermomechanical properties of the samples are not affected by immersion in PBS solution.

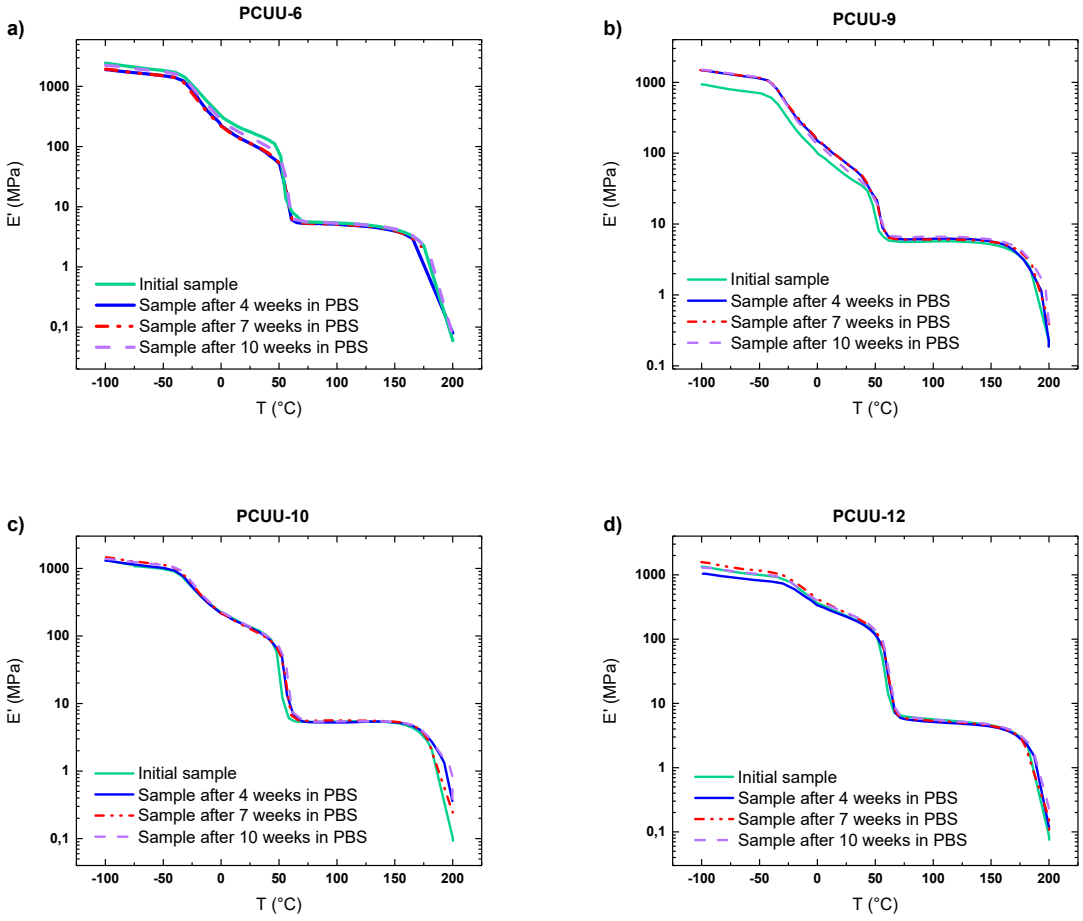

Figure 12. DMTA curves of investigated PCUUs - comparison of initial sample with samples immersed in buffer solutions for various periods of time.

3.5. Mechanical properties

For the investigation of mechanical properties samples after 4 weeks in PBS buffer solutions were used, as well as an additional batch of the samples after 20 weeks of immersion in PBS buffer was analyzed (Table 2). All investigated materials have shown a decrease in Young's modulus (E), tensile strength (σ_b), and elongation at break (ε_b) after 4 weeks of immersion in PBS solutions, much more pronounced in case of PCUU-6 and PCUU-9. However, after 20 weeks, these parameters increased again. Similar behavior was observed in previous reports about PCUUs obtained based on oligo(tetra- and hexamethylene carbonate-urethane)s [2].

Table 2. Mechanical properties of PCUUs determined by tensile test before and after immersion in PBS solution at 37 °C for 20 weeks.

Sample	E (MPa)	σ_b (MPa)	ε_b (%)
PCUU-12	59 ± 9	48 ± 3	730 ± 10
PCUU-12_PBS-4	25 ± 3	33 ± 9	630 ± 30
PCUU-12_PBS-20	78 ± 9	39 ± 8	680 ± 90
PCUU-10	37 ± 2	42 ± 3	850 ± 40
PCUU-10_PBS-4	6 ± 1	31 ± 4	780 ± 30
PCUU-10_PBS-20	49 ± 4	38 ± 2	800 ± 60
PCUU-9	18 ± 6	39 ± 2	810 ± 40
PCUU-9_PBS-4	6 ± 1	26 ± 6	680 ± 50
PCUU-9_PBS-20	10 ± 2	29 ± 6	670 ± 40
PCUU-6	43 ± 7	43 ± 7	890 ± 30
PCUU-6_PBS-4	5 ± 0	24 ± 3	670 ± 60
PCUU-6_PBS-20	35 ± 1	38 ± 5	730 ± 40

A Potential explanation for the changes of mechanical properties of PCUUs could be the hindered-urea dissociation mechanism, in which dissociation of kinetic products and then their reorganization into thermodynamic stable products takes place. Urea bonds are one of the most stable chemical bonds due to the conjugation stabilization effect of its dual amide structure [37]. However, presence of bulky substituents to one of its nitrogen atoms can disturb the orbital co-planarity of the amide bonds, and thus hinder the conjugation effect. Therefore, the decrease of *E* of PCUUs in the first 4 weeks of immersion in PBS buffer could be interpreted as the consequence of hindered-urea dissociation with slightly decreasing molecular weight. In case of PCUU-10 and PCUU-12, an increase of *E* after 20 weeks in PBS in comparison to initial samples was observed. Most probably, after the initial rupture of urea PCUUs regained their modulus through amine-isocyanate addition resulting in formation of new, less congested urea bonding (Scheme 2). Furthermore, an increase of *E* could have been caused also by the increase of the crystalline phase as a result of the annealing process. Tensile strength after 20 weeks decreased in case of all investigated samples, however the remaining σ_b were in the range of 29 to 39 MPa. The ε_b after 20 weeks in PBS solutions decreased only slightly and remained in the range of 670 to 800% in case of PCUU-9_PBS-20, and PCUU-10_PBS-20, respectively (Table 2).

In the IPDI molecule, the secondary isocyanate has a higher reactivity compared to the primary group, which is attributed to the primary group being more sterically hindered by the closely located methyl group. However, the selectivity for the reaction can change depending on the catalyst used. The secondary isocyanate reaction can be enhanced by using dibutyltin dilaurate (DBTDL) as a catalyst, whereas using 1,4-diazabicyclo[2.2.2]octane (DABCO) as a catalyst can invert the reaction to be selective to the primary isocyanate group [38]. Therefore, in the first step of the synthesis of PCUUs the oligo(alkylene carbonate) diols were bonded to more reactive secondary isocyanate of IPDI through the urethane bond, whereas the less

reactive primary isocyanates of IPDI were linked together into urea linkages upon curing. As a result, the urea structures linked to bulky groups (-CH_2-$C(CH_2)_2CH_3$) are expected to be relatively more congested upon the moisture curing stage. In addition, due to high excess of IPDI used in the synthesis, also longer blocks of urea groups can be formed, resulting in urea bonds with non-symmetrical surrounding originating from two different NCO groups (Scheme 2). Therefore, it can be expected that more steric hindered urea bonds shall become unstable in an aqueous buffer solution, and they would undergo dissociation much faster than other urea groups to form the corresponding amine reactive intermediates. As a result, the reorganization of those urea groups will occur with relatively higher rates than those of the rest (Scheme 2).

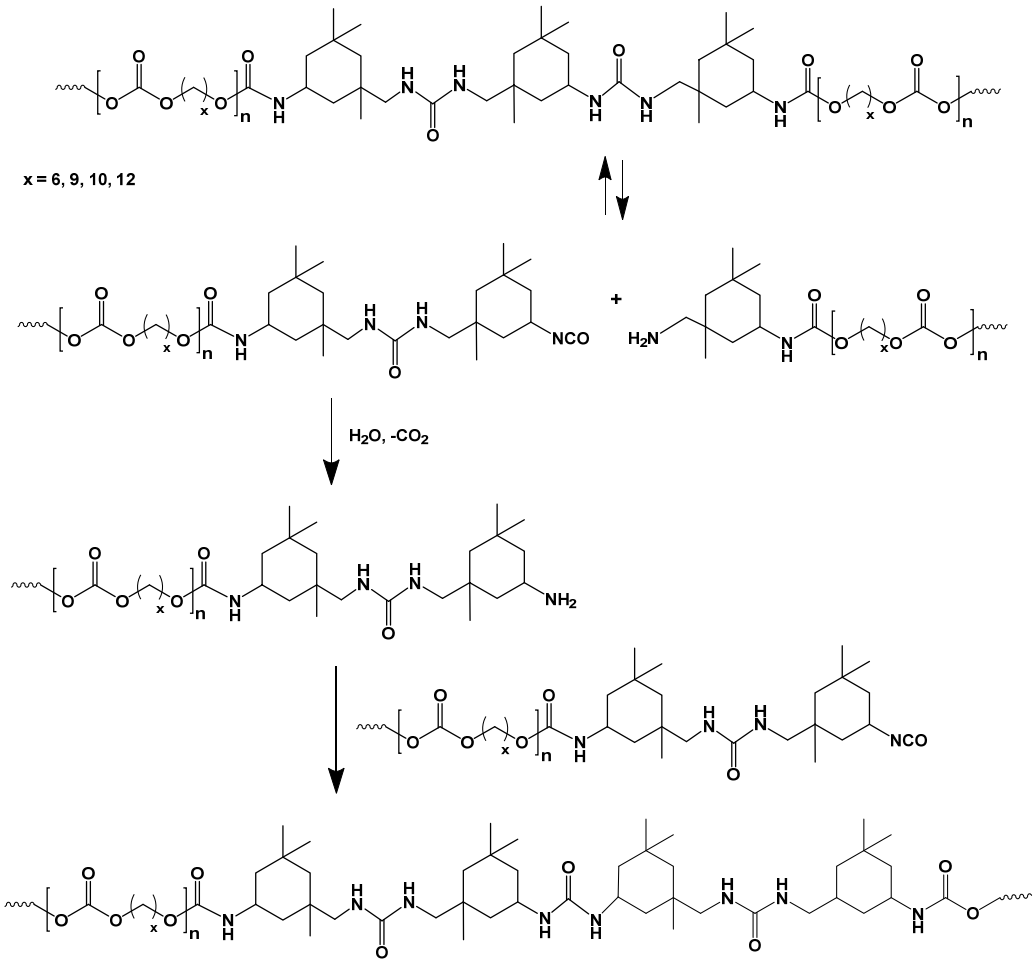

Scheme 2. Hindered-urea dissociation mechanism - rupture of urea PCUUs and amine-isocyanate addition resulting in formation of new, less congested urea bonding.

3.6. Analysis of PBS solutions after immersion

FTIR analysis of buffer solutions was performed to investigate degradation products of PCUUs (Figure 13, exemplarily for samples after 4 weeks in PBS solution and Figure S3, exemplarily for samples after 10 weeks in PBS solution). In the region between 3200 and 3500 cm^{-1} two signals at 3360 and 3197 cm^{-1} were found and assigned to stretching bands of hydrogen-bonded N-H in amines and N-H stretching band of secondary amide. In case of PCUU-6 bands related to N-H groups were much stronger when compared to the other of the samples. In addition, a strong band at 3454 cm^{-1} was detected in the spectrum of PCUU-6, however it is related to contamination with water. The intensity of bands at 1660 and 1635 cm^{-1}, which are characteristic for urea formations, were the strongest in all of the investigated samples. Peaks assigned to carbonate groups (1738 and 1720 cm^{-1}) as well as to urethanes (around 1690 and 1700 cm^{-1}) were also present, however to much a smaller extent. In case of degradation products found in the PBS solutions after 10 weeks of immersion of PCUUs, no signals from urethane or carbonate were detected (Figure S3).

The strong proton signal of NH in urea was also detected by ^{1}H NMR in the range of 5.0-6.0 ppm (Figure 13c). Small signals from NH protons from urethane were visible in the range of 7.0-7.5 ppm, as well as small signals from protons in the neighborhood of carbonate groups at 4.1 ppm.

GPC analyses of solutions did show identical elution diagrams in case of all samples investigated (Figure 14). Average number molecular weights (M_n) were around 700-740 $g \cdot mol^{-1}$, with bi-modal distribution (maxima around 500 and 1100 $g \cdot mol^{-1}$) and dispersity indices around 1.2.

All of these results suggest that most probably the content of the buffer solutions after immersion of the samples could origin from the hard segment decomposition related to the dissociation mechanism of hindered urea bonds within hard segments of PCUUs, according to

which possibly short chains containing longer blocks of hard segments are expected to be formed.

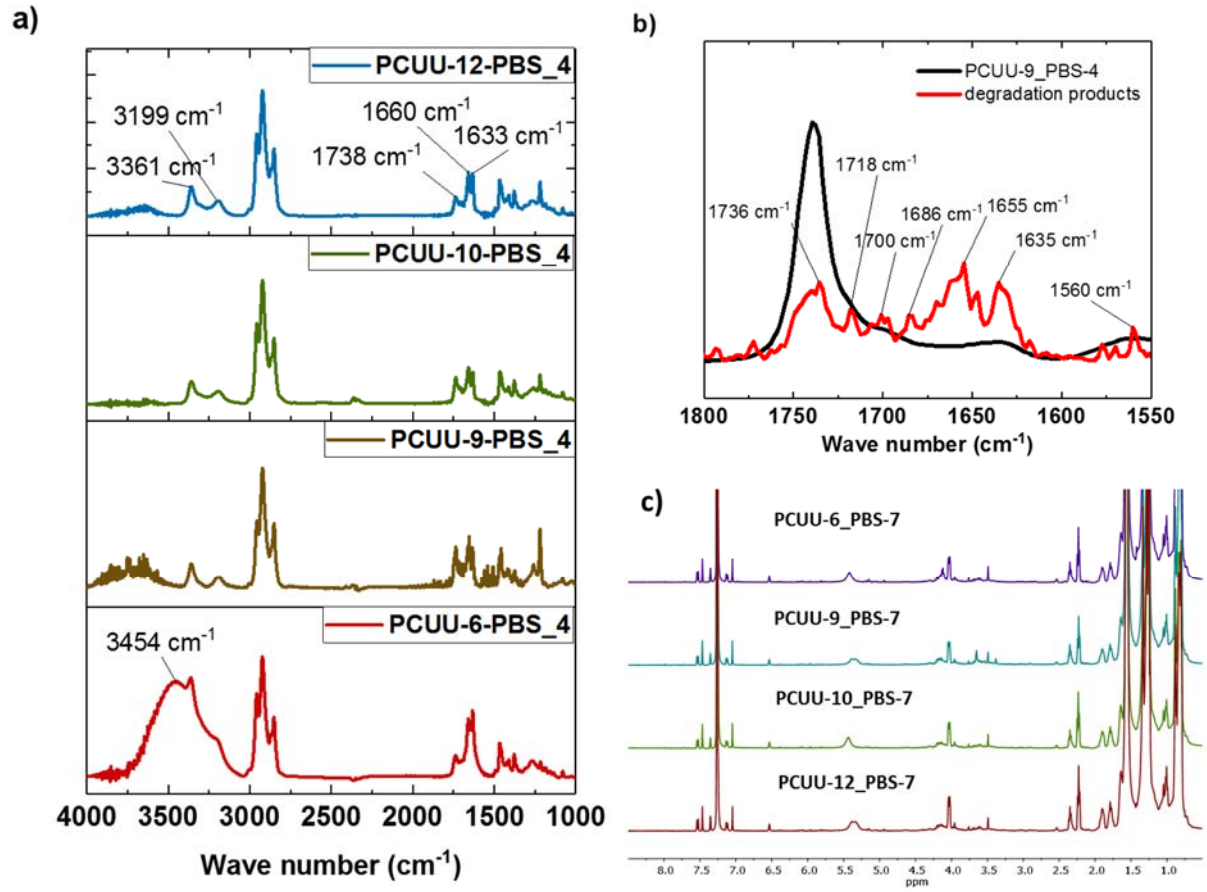

Figure 13. FTIR spectra of the degradation products found in PBS solutions after 4 weeks of immersion (a). FTIR spectra of PCUU-9_PBS-4 and of the degradation products in the wave number range of 1550-1800 cm^{-1} (b). ^{1}H NMR spectra of the degradation products, exemplary for samples after immersion in PBS solutions for 7 weeks (c).

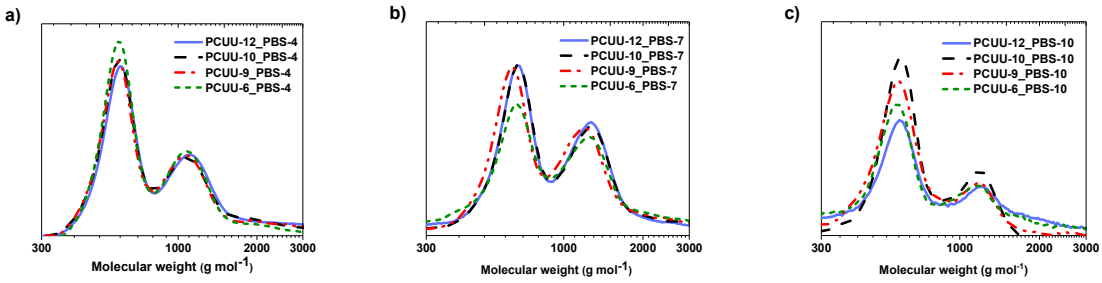

Figure 14. GPC diagrams – results of measurement of oligomers content in buffer solutions for the PCUU samples immersed for 4 (a) and 7 weeks (b), and 10 weeks (c) in PBS.

4. Conclusions

Polycarbonate-based polyurethanes and polyureas are promising implant materials due to the improved resistance to hydrolytic degradation and lower inflammation of the surrounding tissue in comparison to poly(ester-urethane)s. Furthermore, oxidative stability of poly(carbonate-urethane)s was reported to be much higher than in case of poly(ether-urethane)s, attractive candidate-materials for long-term implants. In the present study, we have investigated the influence of the concentration of carbonate units within the soft segments on the hydrolytic stability of the PCUUs. Here, for the first time, PCUUs obtained from oligo(alkylene carbonate) diols containing longer hydrocarbon chains (6, 9, 10, and 12 methylene units) were used for such investigations.

Acknowledgments

This research was financially supported by European Social Fund and Human Capital National Cohesion Strategy Program in Poland within the project number 34/ES/ZS-III/W-POKL/14 and by the Helmholtz-Association through program-oriented funding. We would like also to thank Dr. Karola Lützow for her help with NMR measurements, and Mrs. Susanne Schwanz for technical support with the thermal analysis measurements.

References

[1] M. Serkis, M. Špírková, R. Poręba, J. Hodan, J. Kredatusová, D. Kubies, Hydrolytic stability of polycarbonate-based polyurethane elastomers tested in physiologically simulated conditions, Polym. Degrad. Stab., 119 (2015) 23-34.
[2] J. Kozakiewicz, G. Rokicki, J. Przybylski, K. Sylwestrzak, P.G. Parzuchowski, K.M. Tomczyk, Studies of the hydrolytic stability of poly(urethane–urea) elastomers synthesized from oligocarbonate diols, Polym. Degrad. Stab. , 95 (2010) 2413-2420.
[3] J. Mystkowska, M. Mazurek-Budzyńska, E. Piktel, K. Niemirowicz, W. Karalus, P. Deptuła, K. Pogoda, D. Łysik, J.R. Dąbrowski, G. Rokicki, R. Bucki, Assessment of aliphatic poly(ester-carbonate-urea-urethane)s potential as materials for biomedical application, J. Polym. Res., 24 (2017) 144.

[4] E.M. Christenson, S. Patel, J.M. Anderson, A. Hiltner, Enzymatic degradation of poly(ether urethane) and poly(carbonate urethane) by cholesterol esterase, Biomaterials, 27 (2006) 3920-3926.
[5] I. Khan, N. Smith, E. Jones, D.S. Finch, R.E. Cameron, Analysis and evaluation of a biomedical polycarbonate urethane tested in an in vitro study and an ovine arthroplasty model. Part I: materials selection and evaluation, Biomaterials, 26 (2005) 621-631.
[6] S.-h. Hsu, Z.-C. Lin, Biocompatibility and biostability of a series of poly(carbonate)urethanes, Colloids and Surfaces B: Biointerfaces, 36 (2004) 1-12.
[7] A.M. Seifalian, H.J. Salacinski, A. Tiwari, A. Edwards, S. Bowald, G. Hamilton, In vivo biostability of a poly(carbonate-urea)urethane graft, Biomaterials, 24 (2003) 2549-2557.
[8] C.S. Schollenberger, F.D. Stewart, Thermoplastic polyurethane hydrolysis stability, Angew. Makromol. Chem., 29 (1973) 413-430.
[9] Y.W. Tang, R.S. Labow, J.P. Santerre, Isolation of methylene dianiline and aqueous-soluble biodegradation products from polycarbonate-polyurethanes, Biomaterials, 24 (2003) 2805-2819.
[10] D.K. Dempsey, C. Carranza, C.P. Chawla, P. Gray, J.H. Eoh, S. Cereceres, E.M. Cosgriff-Hernandez, Comparative analysis of in vitro oxidative degradation of poly(carbonate urethanes) for biostability screening, J. Biomed. Mater. Res. Part A, 102 (2014) 3649-3665.
[11] M. Sobczak, C. Dębek, E. Olędzka, G. Nałęcz-Jawecki, W.L. Kołodziejski, M. Rajkiewicz, Segmented polyurethane elastomers derived from aliphatic polycarbonate and poly(ester-carbonate) soft segments for biomedical applications, J. Polym. Sci. Part A: Polym. Chem., 50 (2012) 3904-3913.
[12] B. Ochiai, H. Amemiya, H. Yamazaki, T. Endo, Synthesis and properties of poly(carbonate-urethane) consisting of alternating carbonate and urethane moieties, J. Polym. Sci. Part A: Pol. Chem., 44 (2006) 2802-2808.
[13] S. Baudis, S.C. Ligon, K. Seidler, G. Weigel, C. Grasl, H. Bergmeister, H. Schima, R. Liska, Hard-block degradable thermoplastic urethane-elastomers for electrospun vascular prostheses, J. Polym. Sci. Part A: Polym. Chem., 50 (2012) 1272-1280.
[14] R.S. Labow, E. Meek, J.P. Santerre, Hydrolytic degradation of poly(carbonate)-urethanes by monocyte-derived macrophages, Biomaterials, 22 (2001) 3025-3033.
[15] R. Poręba, M. Špirková, J. Pavličević, J. Budinski-Simendić, K. Mészáros Szécsényi, B. Holló, Aliphatic polycarbonate-based polyurethane nanostructured materials. The influence of the composition on thermal stability and degradation, Composites Part B: Eng., 58 (2014) 496-501.
[16] R. Poręba, M. Špírková, L. Brožová, N. Lazić, J. Pavličević, A. Strachota, Aliphatic polycarbonate-based polyurethane elastomers and nanocomposites. II. Mechanical, thermal, and gas transport properties, J. Appl. Polym. Sci., 127 (2013) 329-341.
[17] M. Špírková, L. Machová, L. Kobera, J. Brus, R. Poręba, M. Serkis, A. Zhigunov, Multiscale approach to the morphology, structure, and segmental dynamics of complex degradable aliphatic polyurethanes, J. Appl. Polym. Sci., 132 (2015) 41590.
[18] M. Špírková, J. Pavličević, A. Strachota, R. Poreba, O. Bera, L. Kaprálková, J. Baldrian, M. Šlouf, N. Lazić, J. Budinski-Simendić, Novel polycarbonate-based polyurethane elastomers: Composition–property relationship, Eur. Polym. J., 47 (2011) 959-972.
[19] J.P. Santerre, K. Woodhouse, G. Laroche, R.S. Labow, Understanding the biodegradation of polyurethanes: From classical implants to tissue engineering materials, Biomaterials, 26 (2005) 7457-7470.
[20] Y.W. Tang, R.S. Labow, J.P. Santerre, Enzyme-induced biodegradation of polycarbonate-polyurethanes: Dependence on hard-segment chemistry, J. Biomed. Mater. Res., 57 (2001) 597-611.

[21] Y.W. Tang, R.S. Labow, J.P. Santerre, Enzyme-induced biodegradation of polycarbonate polyurethanes: Dependence on hard-segment concentration, J. Biomed. Mater. Res., 56 (2001) 516-528.
[22] H.J. Salacinski, M. Odlyha, G. Hamilton, A.M. Seifalian, Thermo-mechanical analysis of a compliant poly(carbonate-urea)urethane after exposure to hydrolytic, oxidative, peroxidative and biological solutions, Biomaterials, 23 (2002) 2231-2240.
[23] M.M. Mazurek, K. Tomczyk, M. Auguścik, J. Ryszkowska, G. Rokicki, Influence of the soft segment length on the properties of water-cured poly(carbonate-urethane-urea)s, Polym. Adv. Technol., 26 (2015) 57-67.
[24] A. Lendlein, A.M. Schmidt, M. Schroeter, R. Langer, Shape-memory polymer networks from oligo(ϵ-caprolactone)dimethacrylates, J. Polym. Sci. A: Polym. Chem., 43 (2005) 1369-1381.
[25] C. Vasile, G.E. Zaikov, Environmentally Degradable Materials Based on Multicomponent Polymeric Systems, CRC Press, Leiden, 2009.
[26] Z. Ying, Y. Dong, J. Wang, Y. Yu, Y. Zhou, Y. Sun, C. Zhang, H. Cheng, F. Zhao, Carbon dioxide as a sustainable resource for macrocyclic oligourea, Green Chem., 18 (2016) 2528-2533.
[27] B. Pilch-Pitera, Polyurethane powder coatings crosslinked with allophanate structures containing polyisocyanates, J. Appl. Polym. Sci., 116 (2010) 3613-3620.
[28] Y. Shi, X. Zhan, Z. Luo, Q. Zhang, F. Chen, Quantitative IR characterization of urea groups in waterborne polyurethanes, J. Polym. Sci. Part A: Polym. Chem., 46 (2008) 2433-2444.
[29] A. Lapprand, F. Boisson, F. Delolme, F. Méchin, J.P. Pascault, Reactivity of isocyanates with urethanes: Conditions for allophanate formation, Polym. Degrad. Stab., 90 (2005) 363-373.
[30] I. Poljanšek, E. Fabjan, D. Moderc, D. Kukanja, The effect of free isocyanate content on properties of one component urethane adhesive, Int. J. Adhes. Adhes., 51 (2014) 87-94.
[31] B.S. Ritter, R. Mülhaupt, Isocyanate- and Solvent-Free Route to Thermoplastic Poly(amide-urea) Derived from Renewable Resources, Macromol. Mater. Eng., 302 (2017) 1600338.
[32] W.-G. Qiu, F.-L. Zhang, X.-B. Jiang, X.-Z. Kong, NMR Analysis to Identify Biuret Groups in Common Polyureas, Chin. J. Polym. Sci., 36 (2018) 1150-1156.
[33] X. Chen, X. Liu, J. Lei, L. Xu, Z. Zhao, F. Kausar, X. Xie, X. Zhu, Y. Zhang, W.Z. Yuan, Synthesis, clustering-triggered emission, explosive detection and cell imaging of nonaromatic polyurethanes, Molecular Systems Design & Engineering, 3 (2018) 364-375.
[34] N. Bialas, H. Höcker, M. Marschner, W. Ritter, 13C NMR studies on the relative reactivity of isocyanate groups of isophorone diisocyanate isomers, Makromol. Chem., 191 (1990) 1843-1852.
[35] S. Jiang, R. Shi, H. Cheng, C. Zhang, F. Zhao, Synthesis of polyurea from 1,6-hexanediamine with CO2 through a two-step polymerization, Green Energy & Environment, 2 (2017) 370-376.
[36] N.M. Girouard, S. Xu, G.T. Schueneman, M.L. Shofner, J.C. Meredith, Site-Selective Modification of Cellulose Nanocrystals with Isophorone Diisocyanate and Formation of Polyurethane-CNC Composites, ACS Appl. Mater. Interfaces, 8 (2016) 1458-1467.
[37] H. Ying, J. Cheng, Hydrolyzable Polyureas Bearing Hindered Urea Bonds, Journal of the American Chemical Society, 136 (2014) 16974-16977.
[38] H.-K. Ono, F.N. Jones, S.P. Pappas, Relative reactivity of isocyanate groups of isophorone diisocyanate. Unexpected high reactivity of the secondary isocyanate group, Journal of Polymer Science: Polymer Letters Edition, 23 (1985) 509-515.